ELSEVIER

Biophysical Chemistry 53 (1994) 155–168

Biophysical Chemistry

Inelastic neutron-scattering study of the proton transfer dynamics in polyglycine I at 20 K

F. Fillaux [a,*], J.P. Fontaine [a], M.H. Baron [a], N. Leygue [a], G.J. Kearley [b], J. Tomkinson [c]

[a] *Laboratoire de Spectrochimie Infrarouge et Raman Centre National de la Recherche Scientifique, 2 rue Henry-Dunant, 94320 Thiais, France*

[b] *Institut Laue-Langevin BP 156 X, 38042 Grenoble Cedex 9, France*

[c] *Rutherford Appleton Laboratory, Chilton, OX11 0QX, UK*

Received 15 November 1993; revised 15 December 1993; accepted 30 December 1993

Abstract

Inelastic neutron-scattering (INS) spectra of three isotopic derivatives of polyglycine I $(-COCH_2NH-)_n$, $(-COCD_2NH-)_n$, and $(-COCH_2ND-)_n$ at 20 K are presented from 30 to 4000 cm^{-1}. The band frequencies are compared to those observed in the infrared and Raman. Assignments in terms of group vibrations are proposed. These mostly resemble previous assignment schemes, except for the amide bands. The INS intensities reveal that the proton dynamics for the (N)H proton are totally different from those proposed previously. They are independent of the molecular frame and the valence bond approach is not consistent with observation. A phenomenological approach is proposed in terms of localized modes. The calculated intensities reveal that the (N)H stretching mode has two components at ~1377 and 1553 cm^{-1}. This is a dramatic change compared to all former assignments at ~3280 cm^{-1} based on infrared and Raman data. These proton-dynamics are associated with a weakening of the N–H bond due to the ionic character of the hydrogen bond ($N^{\delta-}...H^{+}...O^{\delta'-}$) and proton transfer. The infrared and Raman spectra are re-examined and a new assignment scheme is proposed for the amide bands; the amide A and B bands are re-assigned to the overtones of the stretching modes. A symmetric double-minimum potential for the proton is consistent with all the observations.

Keywords: Inelastic neutron scattering; Infrared; Raman; Hydrogen bond; Proton transfer

1. Introduction

The polyglycine (PG) $(-COCH_2NH-)_n$ is the simplest polypeptide and the vibrational dynamics of this polymer has been thoroughly investigated, using infrared and Raman [1–6]. Extensive force-field models have been proposed [6–14]. These studies are of importance for a better understanding of the molecular dynamics of more complicated proteins of biological interest. However, a major problem in force-field calculation based on the infrared and Raman spectra of isotopically substituted molecules is that the number of unknown force constants is normally very much greater than the number of observed frequencies. Therefore, these force fields are not free from some arbitrariness and, in several cases, quite different force fields have been proposed which fit equally well the observations. In principle, this difficulty could be removed by con-

* Corresponding author.

SSDI 0301-4622(94)00086-Y

sidering the infrared and Raman intensities which are related to the eigen-vectors describing the atomic displacements for each mode [15], but the molecular factors required for intensity calculations (the dipole moment in the infrared and the polarizability tensor in Raman) are largely unknown. In contrast to this, inelastic neutron scattering (INS) provides direct information on the eigen-vectors describing the vibrational modes, because intensities are totally determined by the nuclear cross sections and the mean-square displacements of the atoms in each mode. Therefore, dynamical models obtained from optical studies but which produce poor fits to INS data can be eliminated as being irrelevant. In addition, because of the very large cross section of the hydrogen atom, INS spectra of hydrogenous systems are dominated by the protonic modes. On the one hand, this is a great advantage since the band assignment is straightforward, but, on the other, this is also a great limitation because the dynamics of the other atoms remains largely undetermined. Furthermore, whereas only the centre of the Brillouin zone is probed with optical techniques, INS gives the whole density-of-states. This is of importance in the case of polyglycine where significant dispersion for the phonon branches may take place. Finally, INS is unique in observing overtones and combination bands which are usually rather weak in the infrared and Raman, except perhaps for resonance Raman.

Previous study, on the N-methylacetamide molecule (NMA, $CH_3CONHCH_3$) and various methyl-deuterated analogs [16], had shown that INS yields a completely new picture for the proton dynamics and hydrogen bonding. The usual valence-bond approach must be abandoned for the amidic proton which no longer rides the displacements of the nitrogen or oxygen atoms. Instead, the dynamics of the amidic proton are best regarded as independent of the molecular-skeleton modes, as they are in hydrogen-bonded ionic crystals [17]. In addition, the data analysis for the $CD_3CONHCD_3$ derivative revealed that the (N)H stretching mode must be located at $\sim 1575\ cm^{-1}$. The bands at 3250–3100 cm^{-1}, originally thought to be the stretching modes, correspond better to their overtones. These unforeseen proton dynamics were associated with the weakening of the N–H bond due to the ionic character of the hydrogen bond ($N^{\delta-}...H^{+}...O^{\delta\prime-}$) and proton transfer. The infrared and Raman spectra were then reconsidered and a new assignment scheme was proposed for the amide bands in terms of dynamical proton-exchange between the amide-like (...OCNH...) and imidol-like (...HOCN...) forms in infinite chains of hydrogen-bonded molecules.

The leading motivation of the present paper is to see whether the proton dynamics in the simplest polypeptide (i.e. polyglycine or PG) must also be reconsidered. Previous INS studies of the polyglycine were limited by the rather modest energy-transfer range of the spectrometer and statistical quality of the data [9]. Nowadays, one neutron spectrometer provides spectra between 30 and 4000 cm^{-1}, which cover the whole internal-mode region necessary to achieve a thorough dynamical analysis. We have therefore undertaken an INS study of three isotopic derivatives of PG, $(-COCH_2NH-)_n$, $(-COCD_2NH-)_n$, and $(-COCH_2ND-)_n$, at 20 K. This report deals with one particular structure of this polymer: the antiparallel-chain rippled-sheet, usually referred to as PG I. The other structure (triple-helix or PG II) will be reported separately.

In this paper, the INS data and qualitative band assignments in terms of group coordinates are presented in Section 5. In Section 6, localized protonic modes consistent with the INS data are introduced and we propose a new assignment scheme for the amide bands. In Section 7, we re-examine the infrared and Raman spectra. The spectral profiles are consistent with a symmetric double-minimum potential for the stretching mode of the hydrogen bonds. Finally, some outstanding problems are briefly mentioned in Section 8.

2. Experimental

Polyglycine $(-COCH_2NH-)_n$, was purchased from BACHEM. The form I was cast from trifluoroacetic acid (CF_3COOH). The $(-COCH_2ND-)_n$ derivative was obtained in the same way after three exchanges with deuterated trifluoroacetic acid (CF_3COOD). The final deuterium content was $\sim 80\%$ of all possible sites. The $(-COCD_2NH-)_n$ analog was prepared by polymerization of the glycine NH_2CD_2COOH in dimethylsulfoxide in presence of triethylamine and diphenyl phosphoryl azide (DPPA) [18,19]. The polymer was precipitated by adding water saturated with NaCl and then centrifugated. The polymer was washed three times with water, three times with a 5% solution of $KHCO_3$ and, again, three times with water. Finally, the

water was eliminated by washing with acetone, then methanol and then ether. The yield was ~30%. The deuterated glycine was obtained from deuterated acetic acid (CD_3COOD) and trifluoroacetic acid anhydride ($(CF_3CO)_2O$) [20,21]. The deuterium content was greater than 98% of the possible sites.

INS spectra were obtained on the TFXA spectrometer at the ISIS pulsed neutron source, Rutherford Appleton Laboratory, Chilton, UK [22]. The spectra were converted from counts per channel to $S(Q,\omega)$ per cm^{-1} energy transfer by standard programs [23]. The spectrometer has excellent resolution, $\Delta\omega/\omega \leqslant 2\%$. The samples were wrapped in aluminum foil under a dry atmosphere and loaded into a cryostat at 20 K. The spectrum of the empty cryostat was subtracted from the sample spectra.

Infrared spectra of films on BrTi plates were recorded on a Perkin-Elmer 983 spectrometer also at 20 K. Below 200 cm^{-1}, the infrared spectra of Nujol mulls between polyethylene plates were recorded on a Bruker IFS113V spectrometer. Fourier transformed infrared Raman (FTIR) spectra were obtained at room temperature with a 2000R Perkin-Elmer spectrometer using the 1.06 μm line of a Nd:YAG laser. The crystal powders were in sealed glass tubes.

3. Calculation

The INS intensity calculations were performed using the program CLIMAX [24] which produces $S(Q,\omega)$ intensities taking full account of the Debye–Waller factor for fundamentals, overtones and combinations.

4. Crystal structure and symmetry

Two structures have been proposed for PG I: the antiparallel-chain pleated-sheet [25] and the antiparallel-chain rippled-sheet [26,27]. For both structures there are four peptide groups in the unit cell. The pleated sheet structure with D2 symmetry has twofold screw axes parallel to the a ($C_2^s(a)$) and to the b crystal axis ($C_2^s(b)$) and a twofold rotation axis parallel to c($C_2(c)$). The rippled-sheet structure with C_{2h} symmetry has a twofold screw axis parallel to b($C_2^s(b)$), an inversion center i and and a glide plane parallel to (a, c) ($\sigma_{ca}^g(b)$). The distances between two neighboring chain axes in a sheet is ~4.7–4.8 Å. Peptide groups form interchain hydrogen bonds with $R_{N\cdots O} \sim 2.9$ Å. The most important interchain interaction is due to the hydrogen bond. Interaction between chains in neighboring sheets are much smaller.

Each normal mode for the isolated peptide unit gives four phonon branches. The optically active symmetry species, characterized by their phases either along the chains (ϕ) or between chains (ϕ'), are given in Table 1. The main difference between the two structures is due to the inversion centre in the rippled-sheet structure. Therefore, transitions are active either in the infrared (A_u and B_u) or in Raman (A_g and B_g). For the pleated-sheet structure, all the B symmetry species are infrared and Raman active. Overtones are only Raman active for the rippled-sheet and should be totally inactive for the pleated-sheet.

5. INS spectra and band assignments

The INS spectra of the three isotopic derivatives of PG I at 20 K are presented in Figs. 1 to 3. Infrared, Raman and INS band frequencies and assignments in terms of group vibrations are given in Table 2.

As anticipated, the INS spectra of the $(-COCH_2-NH-)_n$ (Fig. 1) and $(-COCH_2ND-)_n$ (Fig. 3) analogs are dominated by the bands due to the CH_2 entities (see Table 2). Only the latter survive for the N-deuterated sample. The ($-COCD_2NH-$) derivative, on the other hand, is dominated by the bands due to the peptidic proton. A rapid comparison of the spectra reveals that most of the intensity of the skeletal modes at 550–650 cm^{-1} (amide IV and VI) and 200–220 cm^{-1} (amide VII) and of the density-of-states below 200 cm^{-1} (lattice modes) is due to the riding effect of the CH_2 protons. All these modes are weak for the $(-COCD_2-NH-)_n$ derivative (Fig. 2). This is similar to the spectrum of potassium hydrogen carbonate ($KHCO_3$) [17] and to NMA crystals at low temperature [16]. Therefore, as for the NMA molecule, the dynamics of the proton engaged in hydrogen bonding are virtually independent of the skeletal modes. This is in marked contrast to the normal modes derived from previous force-field calculations [5].

For a complete analysis of the dynamics in terms of a force-field, it would be necessary to consider two subsystems. Firstly, the backbone with the CH_2 protons

Table 1
Symmetry species and selection rules for polyglycine I

Species	$\nu(\phi, \phi')$	Symmetry			Number of modes	Activity
		$C_2^s(a)$	$C_2^s(b)$	$C_2(c)$		
pleated-sheet (D2)						
A	$\nu(0, 0)$	1	1	1	21	R
B1	$\nu(0, \pi)$	−1	1	−1	20	R, IR (‖)
B2	$\nu(\pi, 0)$	1	−1	−1	20	R, IR (⊥)
B3	$\nu(\pi, \pi)$	−1	−1	1	20	R, IR (⊥)
Species	$\nu(\phi, \phi')$	Symmetry			Number of modes	Activity
		$C_2^s(b)$	i	$s_{ca}^g(b)$		
rippled-sheet (C2h)						
Ag	$\nu(0, 0)$	1	1	1	21	R
Au	$\nu(0, \pi)$	1	−1	−1	20	R, IR (‖)
Bu	$\nu(\pi, 0)$	−1	−1	1	19	R, IR (⊥)
Bg	$\nu(\pi, \pi)$	−1	1	−1	21	R

(‖) Dichroism parallel to the chain axis; (⊥) dichroism perpendicular to the chain axis.

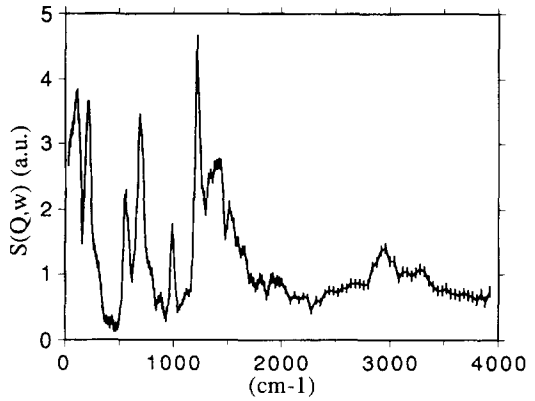

Fig. 1. Inelastic neutron-scattering spectrum of polyglycine I $(-COCH_2NH-)_n$ at 20 K.

to account for the riding effect and, secondly, the peptidic proton in a potential fixed with respect to the crystal frame. This is readily modeled with very heavy masses (say 1000 amu) appropriately located around the protons in order to preserve the local symmetry. The (N)H coordinates are then defined with respect to these masses. In the absence of off-diagonal force-constants the resulting normal modes correspond to pure protonic displacements. They are referred to as 'localized' protonic-modes. In principle, the two dynamical subsystems must be superimposed to allow for possible coupling. However, this paper concentrates on the dynamics of the peptidic proton treated totally independently of the backbone. This approximation will be referred to as the 'proton in a box' model. The normal mode analysis of the backbone is beyond the scope of this paper.

6. The N–H dynamics

The INS spectrum of the $(-COCD_2NH-)_n$ derivative gives a straightforward identification of the NH modes which appear in three distinct frequency ranges.

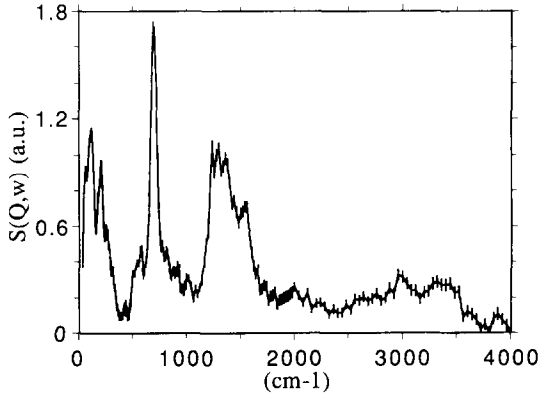

Fig. 2. Inelastic neutron-scattering spectrum of polyglycine I $(-COCD_2NH-)_n$ at 20 K.

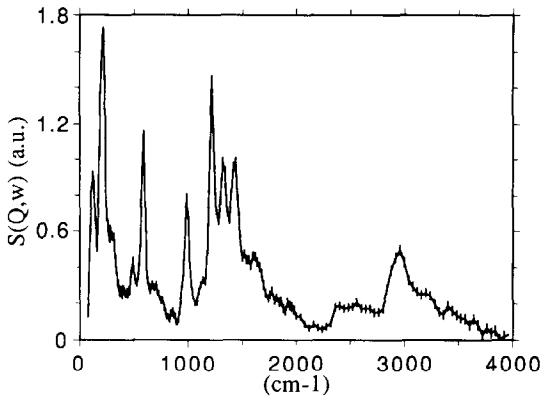

Fig. 3. Inelastic neutron-scattering spectrum of polyglycine I $(-COCH_2ND-)_n$ at 20 K.

According to the usual assignment scheme, we can distinguish in Fig. 2 the out-of-plane bending (γ NH or amide V) at 695 cm^{-1}; the in-plane bending (δ NH or amide II and III) between 1200–1600 cm^{-1} and the stretching (ν NH or amide A and B) between 2900–3400 cm^{-1}. All these modes are very localized.

In INS, there are no symmetry forbidden transitions and the intensity of a mode is a maximum at the frequencies corresponding to the maxima of the proton density-of-states, provided the phonon-wings are small. The γ NH band shows no resolved structure in INS and the frequencies measured with INS and infrared are virtually identical (see Table 2). Therefore, the frequency dispersion is less than the observed bandwidth (full width at half height ~ 70 cm^{-1}) and the coupling between peptide units can be ignored for this mode.

In the 1200–1600 cm^{-1} region five submaxima can be distinguished (Fig. 2 and Table 2). In the previous interpretation of the amide bands, the δ NH and $\nu C=N$ coordinates both contribute to the amide II and III bands of PG I [5]. These bands peak in the infrared at ~ 1520 and 1300 cm^{-1}, respectively. Accordingly, the integrated INS intensities for the in-plane (say between 1100 and 1700 cm^{-1}) and out-of-plane (say between 600 and 800 cm^{-1}) regions should be approximately equal. However, the overtone of the γ NH gives also some intensity ($\sim 70\%$ of the fundamental) [28]. Therefore, the anticipated intensity ratio is $I_{\delta NH}/I_{\gamma NH} \sim 1.7$. However, the observed value, $I_{1200-1600}/I_{600-800} \sim 2.6$, is much greater. Consequently, there is an other protonic mode in this region, and this can only be the stretching mode. With this assignment scheme the calculated intensity ratio (2.7) is quite close to observation. Therefore, as for the NMA molecule, it must be accepted that the fundamental transition for the stretching mode is in the amide II region, whilst the amide A and B bands correspond to overtones.

The proposed assignment scheme is: first, the submaxima at 1240 and 1303 cm^{-1} correspond to the δ (N)H mode. Because of the high degree of deuteration for the $(-COCD_2NH-)_n$ analog, the band at 1240 cm^{-1} does not correspond to the CH bending of non totally deuterated peptide units. (This band at 1222 cm^{-1} is the most intense for the CH_2 analogs, see Figs 1 and 3.) Second, the shoulder at 1450 cm^{-1} is tentatively assigned to the overtone of the γ (N)H and, third, the remaining bands at 1553 and 1377 cm^{-1} are the ν (N)H modes. The splitting of this mode is supported by the splitting of the overtones (amide A and B in the 2900–3300 cm^{-1} region).

This new assignment scheme is supported by the calculation of the INS spectrum of the 'proton in a box' model (Fig. 4). Each mode is split into two components, which are not resolved for the γ (N)H, and phonon-wings are ignored. This is clearly relevant for the γ (N)H band, and the calculation confirms that this is also true for the other modes. The weak broad band at ~ 2000 cm^{-1} is due to the combination of the γ (N)H and ν (N)H modes. However, the overtones of the ν (N)H modes are calculated at ~ 2700–3100 cm^{-1}, whilst the amide A and B bands are observed at ~ 3000–3300 cm^{-1}. This discrepancy is due to the anharmonicity of the actual potential (see below), which is not included in the intensity calculation. Calculated spectra with alternative assignments for the γ (N)H overtone (e.g., 1377 cm^{-1} instead of 1450 cm^{-1}) are much less satisfactory.

7. Discussion

The localized nature of the (N)H modes and the new assignment scheme we propose are the most salient points of this work. They require a thorough re-examination of the infrared and Raman spectra. Before this, however, it is worth comparing the INS spectra of PG I and NMA.

Table 2
Infrared, Raman and INS band frequencies and assignments for the three isotopic-derivatives of PG I. S: strong; m: medium; w: weak; v: very; sh: shoulder; comb.: combination. * new assignment

$(-COCH_2NH-)_n$				$(-COCD_2NH-)_n$				$(-COCH_2ND-)_n$				
Infrared	Raman	INS	assignment	infrared	Raman	INS	assignment	infrared	Raman	INS	assignment	
3283S	3298w	3334w	$2\times\nu$(N)H *	3290S	3298m	3377w	$2\times\nu$(N)H *		3090w		$2\times\nu$(N)H *	
3080w	3090vw	3147vw		3060w	3075w							
2975sh	2973m		$2\times\nu$(N)H *			2996w	$2\times\nu$(N)H *			2977m		
	2933m	2954m	+		2953m			2957sh	2954m		νCH_2	
2927w	2929S		νCH_2	2920w	2926mw			2922S	2927S			
2860vw	2867w		comb.		2867w			2880w	2870sh		comb.	
								2465S	2454m		ν(N)D *	
								2418S	2420sh			
					2207w							
					2173m		νCD_2					
					2158m							
					2123S							
1675sh	1670S			1675sh				1675sh				
	1650sh	1654w	amide I		1668S		amide I		1660S		amide I	
1628S				1624S				1625S		1625w		
						1553m	ν(N)H *					
1528S	1520w	1529m	ν(N)H *	1518S	1515w		+	1480m	1497sh		$\nu C=N$	
	1457S		$+\delta CH_2$			1450w	$\nu C=N$	1440m	1449S	1438m	+	
1430S	1430m	1426m	$+\nu C=N$	1440w	1451m		+	1430sh	1420sh		δCH_2	
	1415m		$+2\times$		1436w	1377m	$2\times$					
1405sh	1405sh	1400sh	γ(N)H *	1370vw	1380vw		γ(N)H *					
1334w	1330sh	1341m	w CH_2					1358m	1325w	1341m	w CH_2	
1290sh	1300w				303m	1303m						
	1281w		δ(N)H	1290w	276sh		δ(N)H					
1255sh	1258w		+		233m	1340						
1235m	1228m		tw CH_2									
1222m	1220sh	1225S							1230m	1222S	tw CH_2	
1215m			νNC	1200mS	1184w		νNC	1200m			νNC	
1180m			+	1180sh			+	1185sh			+	
1150sh	1157		νCC				νCC	1140m	1152m		νCC	

				1090w	1107m		δCD_2					
					1050S		+					
				1015w	1005w		w CD_w					
1030m	1030sh							1030m				
1061mS	1016S		rCH_2					1016mS	1016S		rCH_2	
990w		989m						1000w		995m		
								949m	958m		δ(N)D	
985w	902w			925w	924w	916vw			928vw			
890w	888w	874vw	νNC,CC	890vw			νNC,XX		890vw		νNC,CC	
	867w			865w	870w		+ tw CD_2		870w			
					840m			840m	840w	856vw		
725mS				718m	728w		rCD_2					
705sh	695w	649S	γ(N)H *	705sh		695S	γ(N)H *					
628w			amide IV					621w	618m		amide IV	
605m	596	588sh	+	540w	552nw		amide IV	610w		592m	+	
590nm		557m	amide VI	575w		581w	amide VI	568m	550w		amide VI	
								512S	524mw	489w	γ(N)D *	
355w			comb.	350w	328sh		comb.	345w	350sh		comb.	
320w	329mw	320sh		320w	333mw	320vw		320w	325w	296vw		
270w	284w		$\delta NC^{\alpha}C$	267m	254w	257w	δNC^{α}	270m	250w		$\delta NC^{\alpha}C$	
217m	210w	217S	$\delta C^{\alpha}CN$	222m		206mw	δC^{α}	225m		217S	$\delta C^{\alpha}CN$	
			δCNC^{α}	186^{m}			δCNC^{α}				δCNC^{α}	
	176w		$\tau C=N$				$\tau C=N$	170sh	169m		$\tau C=N$	
140m	146w		τN-b1C	145m			τN–C	142m			τN–C	
	127w		τC–C				τC–C				τC–C	
	114w	120S	Lattice		118m	115m	Lattice		110m	109S	Lattice	

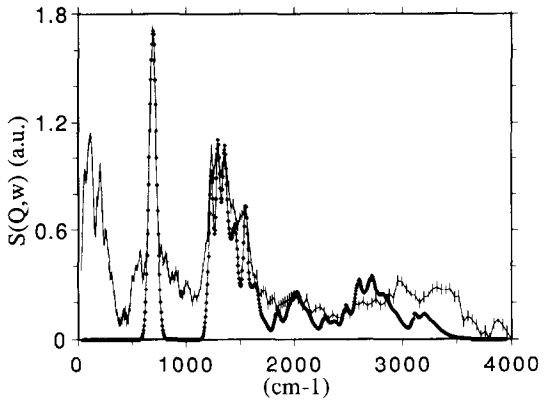

Fig. 4. Comparison of the observed (error bars) and calculated (with the 'proton in a box' model) Inelastic neutron-scattering spectra of polyglycine I ($-COCD_2NH-$) at 20 K.

7.1. Comparison with NMA

For the normalized INS spectra of PG I $(-COCD_2NH-)_n$ and NMA ($CD_3CONHCD_3$) (Fig. 5) the γ (N)H bands have similar integrated intensities, although the band is broader for the polymer, which is less crystalline than NMA. The two spectra reveal great differences in the 1100–1400 cm^{-1} region. The δ (N)H mode which peaks at 1327 cm^{-1} for NMA is shifted to 1303 cm^{-1} in PG I. The ν (N)H mode at 1575 cm^{-1} in NMA is also shifted downwards, to 1553 cm^{-1} in PG I. The overtones of the γ (N)H modes are at similar frequencies for the two systems (i.e. ~1450 cm^{-1}), and it is obvious that the bands at 1377 and 1240 cm^{-1} in PG I have no counterparts in NMA. This confirms that the stretching and in-plane bending

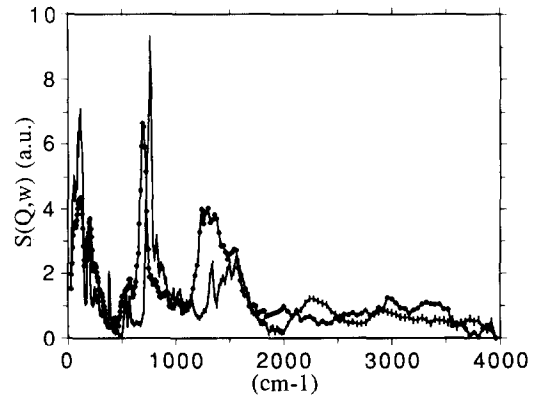

Fig. 5. Comparison of the normalized Inelastic neutron-scattering spectra of polyglycine I $(-COCD_2NH-)_n$ (*) and N-methylacetamide ($CD_3CONHCD_3$, error bars) at 20 K.

Scheme 1.

modes have single components in NMA and two components in PG I.

In our previous work on the NMA crystal [16] the proton dynamics were represented as a dynamical proton exchange between two entities. These entities were tentatively represented as in Scheme 1.

This representation of the single or double bond-characters is extremely schematic. In the NMA crystal at low temperature, the imidol-like form, Y, is largely dominant whilst the two forms are almost equally probable at room temperature. The reaction-path for the interconversion of the two forms is likely to be close to the protonic stretching-coordinate. The proton-transfer dynamics would then be represented as a double-minimum potential-function which is asymmetric at low temperature, and symmetric at room temperature. This was tentatively related to the collective nature for the proton transfer in the infinite chains of hydrogen-bonded molecules.

In PG I the two INS components of the ν (N)H mode suggest that the two entities remain equally probable even at low temperature and the double minimum potential is symmetric. The proton is totally delocalized between the two wells. The distinction between the two entities X and Y (see above) is no longer relevant and the real structure is intermediate. Consequently, compared to the harmonic single well, each level splits into two sub-levels, either symmetric (lower) or anti-symmetric (upper). They are labeled with quantum numbers n^+ and n^-, respectively. In INS there is no symmetry-related selection rule and for a spectrometer of the *TFXA*-type the $0^+ \rightarrow 1^+$ and $0^+ \rightarrow 1^-$ transitions have similar intensities. They may thus correspond to the bands at 1377 and 1553 cm^{-1}, respectively.

7.2. Comparison with the infrared and Raman spectra

This comparison is essential to achieve a consistent description of the vibrational dynamics in PG I. The main interest is that the same vibrations are observed with all three techniques, but with different intensities. With optical techniques only transitions at the centre of the Brillouin zone are observed. The symmetric dou-

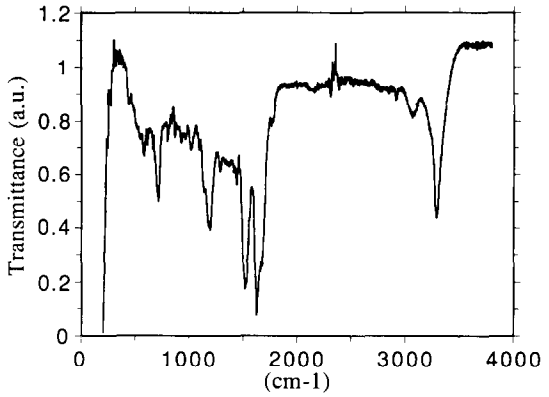

Fig. 6. Infrared spectrum of polyglycine I $(-COCD_2NH-)_n$ at 20 K. Film on a BrTl plate.

ble-minimum potential will give symmetry related selection rules in the infrared and Raman. Only transitions between levels with opposite symmetry are active in the infrared. (Here we consider only the first-order term of the transition moment which is proportional to the first derivative of the dipole moment with respect to the coordinate: $d\mu/dR$.) In Raman, only transitions between levels with the same symmetry can be observed.

The amide I, amide II, amide III and amide V bands

The infrared spectrum of PG I $(-COCD_2NH-)_n$ shows two prominent bands : the amide I which splits into two components at 1675 and 1624 cm^{-1}, and the amide II at 1518 cm^{-1} (see Fig. 6). The usual assignment for the former is predominantly to a $\nu C=O$ mode [5]. The Au–Bu splitting (51 cm^{-1}) is due to dipole–dipole coupling. In Raman, the amide I band is a rather broad and asymmetric peak at $\sim$1665 cm^{-1}, with no resolved structure at room temperature (see Fig. 7). The amide II mode is normally described as an out-of-phase vibration of the ν C=N and δ NH coordinates [5]. It peaks at 1518 cm^{-1} in the infrared but there is no evidence for any Au–Bu splitting. This is surprising since dipole–dipole coupling calculations give almost the same value ($\sim$60 cm^{-1}) as for the amide I band. The amide II mode gives a weak band at 1515 cm^{-1} in Raman.

The amide III mode is a mixture of many different internal coordinates including the δ NH [5]. It is extremely weak in the infrared at 1290 cm^{-1} and shows moderate intensity in Raman at 1303, 1276 and 1233 cm^{-1}. The amide V mode is predominantly represented as the τ CN coordinate with a much smaller γ NH contribution [5]. Its intensity is rather modest in the infrared, at 718 cm^{-1}, and very weak in Raman.

In our assignment scheme, the amide I is still a C=O stretching mode, but here it is completely separated from the (N)H modes. It shows no INS intensity for $(-COCD_2NH-)_n$ (Fig. 2). The weak INS intensity of this mode for the $(-COCH_2NH-)_n$ (Fig. 1) and $(-COCH_2ND-)_n$ (Fig. 3) derivatives, however, reveals some mixing with the CH_2 coordinates. The dynamical separation of the C=O and (N)H modes is also in line with the very weak isotopic shift ($\sim$3 cm^{-1}) of the amide I band for the $(-COCH_2ND-)_n$ analog, compared to $(-COCH_2NH-)_n$ (see Table 2).

Within the symmetric double-minimum picture, the amide II band at 1518 cm^{-1} in the infrared corresponds to the ν (N)H $0^+ \rightarrow 1^-$ transition (this is infrared active) observed at 1553 cm^{-1} in INS. As anticipated, the INS band at 1377 cm^{-1}, which is assigned to the ν (N)H $0^+ \rightarrow 1^+$ transition, has virtually no counterpart in the infrared. There is a very weak band in Raman at $\sim$1380 cm^{-1} which might correspond to the $0^+ \rightarrow 1^+$ transition. The frequency difference between the $0^+ \rightarrow 1^-$ transition observed in INS and in the infrared (1553–1518 = 35 cm^{-1}) compares with the band widths for both techniques. This again points to little frequency dispersion from proton–proton coupling.

In the alternative model, with significant proton–proton coupling, the INS band at 1377 cm^{-1} which is very weak in optical techniques might be assigned to a maximum in the density-of-states, located off-centre of the Brillouin zone. The optical bands at 1515 cm^{-1} would then correspond to a Brillouin zone–centre tran-

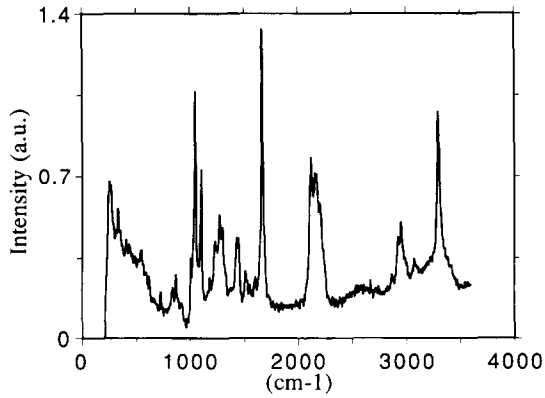

Fig. 7. Raman spectrum of polyglycine I $(-COCD_2NH-)_n$ at room temperature.

sition and the INS band at 1553 cm^{-1} to a nearby maximum of the density-of-states. Although it is not possible to reject one of these two approaches at the present stage a detailed examination of the overtone region (amide A and B, see below) does not support this later assignment scheme.

Our calculations suggest that the nature of the virtually pure δ (N)H amide III mode is basically the same for NMA and PGI. The very weak infrared intensity of this δ (N)H mode for PG I (observed at 1303 and 1240 cm^{-1} in INS) is in marked contrast to NMA [16] where it is observed strongly in INS and infrared. We interpret this lack of intensity for the amide III band of PG I in the infrared as a symmetry related extinction effect. However, within the unit cell containing four peptide units, this mode should give symmetry species with infrared activity for any of the two structures (pleated- or rippled-sheet, see Table 1). Therefore, the selection rule cannot be due to the crystal symmetry. Rather we believe that the infrared extinction is a consequence of the symmetric double-minimum well for the stretching mode. In the ground-state the vibrational wavefunction is symmetric with respect to the double-well centre and the proton is totally delocalized. The in-plane bending of this delocalized proton must be symmetric, as well, and, consequently, inactive in the infrared. In principle it should be Raman active and the bands at 1303, 1270 and 1233 cm^{-1} may correspond to this mode. However, the origin of the splitting into three components is not yet clear.

The nature of the pure γ (N)H amide V mode is also identical for NMA and PG I, but the intensity in the infrared is much weaker for the polymer. As for the in-plane bending mode, this is related to the delocalization of the proton in the symmetric double-well of the stretching mode. However, the greater amplitude of the out-of plane bending (compared to the in-plane bending) favors high-order terms of the dipole moment operator and the infrared extinction is partially relaxed in this case, (e.g., $d^2\mu/dR^2$ gives infrared intensity for transitions between levels with the same symmetry). This band is not observed in Raman.

The amide A and amide B region

In the infrared, the $(-COCD_2NH-)_n$ analog of PG I has a rather intense band at 3290 cm^{-1}. This is the amide A band previously assigned to the fundamental transition of the ν NH mode. A weaker band at 3060 cm^{-1} and an extremely weak band at 2920 cm^{-1} are also observed (see Fig. 6 and Table 2). The relative intensities are reversed in Raman: the bands at 2953–2926 cm^{-1} are rather intense (see Fig. 6 and Table 2). It is now straightforward to assign the amide A band which is intense in the infrared to the ν (N)H $0^+ \rightarrow 2^-$ transition. The weak bands at 3060 (infrared) or 3075 cm^{-1} (Raman) are assigned to combination bands. The bands at $\sim$2950 cm^{-1} which are very weak in the infrared and intense in Raman are assigned to the ν (N)H $0^+ \rightarrow 2^+$ transition. The relative infrared and Raman intensities provide a very strong support for the existence of a centre of symmetry in the proton potential, eventhough the symmetry related selection rules are partially relaxed by partial disorder in the crystal. The Raman intensity at 2950 cm^{-1} for the $(-COCD_2NH-)_n$ analog cannot be explained by a Fermi resonance. In addition, the alternative assignment for the INS band at 1377 cm^{-1} to a Brillouin zone off-centre transition (see above) is not consistent with the Raman spectrum; its overtone should not be observed with the optical spectroscopy techniques.

The frequencies of the $0^+ \rightarrow 2^-$ and $0^+ \rightarrow 2^+$ transitions of the ν (N)H mode are greater than twice the frequencies of the fundamentals (e.g., $2 \times 1553 = 3106$ cm^{-1}, and $2 \times 1377 = 2754$ cm^{-1}). The potential is anharmonic in that it is much steeper than usual.

7.3. *Crystal field symmetry*

In previous interpretations of the infrared and Raman spectra of PG I, the crystal field symmetry and dipole–dipole coupling between the carbonyl groups are supposed to play an important role in splitting the amide I band (1675–1624 cm^{-1} in the infrared, 1668 cm^{-1} in Raman) [5]. However, a similar splitting calculated for the amide II band ($\sim$60 cm^{-1}) is not observed. In our model, the double-minimum for the (N)H stretching mode implies that the levels associated with the chain modes should also split into symmetric and antisymmetric sublevels. This splitting should be related to small changes of the bond-length during the proton transfer. Therefore, the infrared bands are then assigned to the $0^+ \rightarrow 1^-$ (1675 cm^{-1}) and $0^- \rightarrow 1^+$ (1624 cm^{-1}) transitions, and the Raman band at 1668 cm^{-1} to the non-resolved $0^+ \rightarrow 1^+$ and $0^- \rightarrow 1^-$ transitions. If the ground-state splitting is small the 0^- level remains populated even at very low temperature and

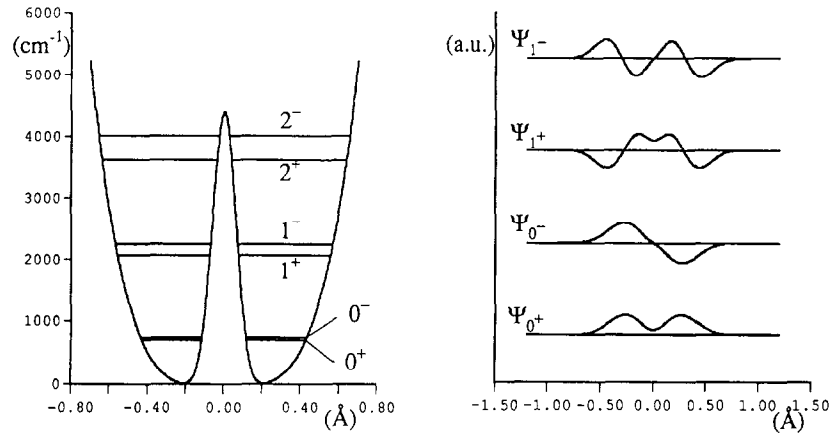

Fig. 8. Double minimum potential function and vibrational wavefunctions for the (N)H stretching mode in polyglycine I.

the transitions should have similar intensities in the infrared ($0^+ \rightarrow 1^-$ at 1675 cm^{-1} and $0^- \rightarrow 1^+$ at 1624 cm^{-1}) or in Raman ($0^+ \rightarrow 1^+$ and $0^- \rightarrow 1^-$ unresolved at 1668 cm^{-1}). It is also possible that this tunnelling-related splitting and the dipole–dipole coupling effect occur simultaneously.

The same approach may explain the splitting of the δ (N)H (amide III) band observed in INS at 1303 and 1240 cm^{-1}. It would correspond to a small change of the NHO angle during the proton transfer. The absence of observable splitting for the γ (N)H (amide V) band, on the other hand, implies that this coordinate is not involved in the proton transfer trajectory.

7.4. *Proton transfer*

The localized nature of the proton dynamics in PG I revealed by the present INS spectrum analysis is comparable to the previous conclusion with NMA and can be interpreted similarly. The local intramolecular interactions related to covalent bonds vanish and are superseded by the mean field arising from long-range interactions in the crystal. Such localized protonic modes were first shown in the INS spectrum of $KHCO_3$ [17] where they were supposed to stem from the ionic nature of the crystal. The localized modes for the peptidic proton reveal a strong ionic character for the hydrogen-bonded molecules in the crystals, though either PG I or NMA crystals are normally regarded as molecular in nature.

Another similarity between PG I and NMA is the very low frequency for the (N)H-stretching modes. According to the correlation of infrared ν NH frequencies and crystallographic $R_{N...O}$ data for various N–H...O systems [29], a stretching frequency at $\sim$3300 cm^{-1}, as previously assigned, was consistent with the N...O distance of $\sim$2.90 Å in PG I or 2.82 Å in NMA [30]. However, this correlation is only correct for systems of the same structure where the proton is covalently bound to the nitrogen atom and the hydrogen-bonding perturbation does not break the N–H bond. The stretching frequency below 1600 cm^{-1} imposes a great weakening of the covalent bond for the proton and it becomes irrelevant to consider the proton as still bound specifically to either atom. The relevant picture becomes $N^{\delta-}...H^+...O^{\delta'-}$, similar to the strong $O^{\delta-}...H^+...O^{\delta-}$ hydrogen bonds [31].

If the very small contribution of the ν CO and δ (N)H coordinates to the proton transfer trajectory are neglected, the effective mass for the stretching mode is 1 amu and a potential function consistent with the observed frequencies is

$$V(x) = 22015\,x^4 + 4446.7\,\exp(-130.1\,x^2). \qquad (1)$$

The distance between the two minima is $\sim$0.4 Å, the potential barrier is $\sim$4400 cm^{-1} (13.2 kcal.mol^{-1}) and the 0^+–0^- level splitting is $\sim$50 cm^{-1} (this is the tunnelling frequency, see Fig. 8). This potential function compares well with that previously proposed for NMA at room temperature, with a barrier height of 7100 cm^{-1} and a tunnel splitting of 32 cm^{-1}. The distances between the two minima are similar for the two systems.

An important consequence of the double-minimum potential is that 'fundamental' and 'overtone' transitions have intensities which are of the same order of

magnitude in the infrared, in agreement with the observation, even if the electrical anharmonicity is negligible. This is a strong argument for rejecting the harmonic approximation where overtones are normally not active. In Raman, however, the electrical anharmonicity is quite large since the overtones are much more intense than the fundamentals.

The energy levels calculated with the same potential (Eq. (1)) for the ν (N)D mode are: 8.4 (0^-), 985 (1^+), 1018 (1^-), 2134 (2^+) and 2238 (2^-) cm^{-1}. The main consequence of the deuteration is the dramatic decrease of the tunnel splitting. Therefore, the 0^- level should be significantly populated, even at 20 K and the corresponding transitions should be observed. However, the 1^+ and 1^- levels cannot be identified safely in the infrared. A skeletal modes occur at 1016 cm^{-1} and the δ (N)D mode is at 949 cm^{-1}. In the overtone region, on the other hand, there are partially resolved bands at 2418 and 2463 cm^{-1} in the infrared, 2420 and 2454 cm^{-1} in Raman. This is consistent with a tunnel splitting of ~ 11 cm^{-1}, closed to the calculated value, but the 2^+–2^- level splitting of ~ 34 cm^{-1} is much smaller than the value of ~ 100 cm^{-1} calculated with Eq. (1). Therefore, a significant change of the potential function appears to take place upon deuteration. In addition, it is impossible to adjust an acceptable double minimum potential analogous to Eq. (1) with the present assignment. The potential barrier would be so high and narrow that its physical relevance is questionable. It is more likely that for the N deuterated PG I the lack of intensity in the infrared region ~ 1000 cm^{-1} means that the 1^+ and 1^- levels are elsewhere and may correspond to the transitions at ~ 2400 cm^{-1}. Potential functions consistent with this assignment are:

$$V(x) = 40234\,x^2 + 12695\,\exp(-196.1x^2), \text{ or}$$

$$V(x) = 0580\,x^4 + 17173\,\exp(-428.6\,x^2). \qquad (2)$$

For both functions, the distance between the two minima is ~ 0.3 Å and the barrier height is greater than 10000 cm^{-1} (30 kcal.mol^{-1}). Even in this case, the physical meaning of such high and narrow barriers is questionable.

8. Outstanding problems

The new aspects of the vibrational dynamics in PG I revealed by INS raise several problems which have not been addressed in this study. Some of them are briefly outlined in this section.

The theoretical framework used in this paper for the localized dynamics is far from satisfactory. Heavy masses, new dynamical subsystems and vibrational coordinates are arbitrarily defined. This phenomenological approach is rather frustrating since contact with the physical and chemical quantities (i.e. forces and bonds) is lost. However, force-field calculations on a more realistic model of the crystal do not avoid the need to separate the (N) proton dynamics from the other degrees of freedom. This is a constraining consequence of the great INS intensity of these proton modes, compared to the backbone vibrations. Therefore, previous force fields proposed on the basis of optical spectra do not lead to a satisfactory representation of the (N)H dynamics. The CH_2 protons, on the other hand, rides the backbone vibrations and a full force-field calculation is necessary to describe their dynamics.

The existence of dynamical proton transfer along the hydrogen bond in PG I is the central point in this work. The analysis of the INS spectra and the selection rules in the infrared and Raman give a convincing evidence of this. However, the tunnelling transition anticipated at ~ 50 cm^{-1} is not observed. This contrasts to some other systems where tunnelling transitions in the same frequency range give intense and narrow INS bands readily observed with the TFXA spectrometer [32,33]. The lack of intensity for the tunnelling transition in PG I casts some doubt on the distance between the two minima of the potential function Eq. (1). However, two effects may depress the intensity of the tunnelling transition in PG I. Firstly, the PG I crystal is rather disordered and the tunnelling band may be very broaden. Secondly, the intensity of the tunnelling transition varies rapidly with the kinetic momentum transfer (Q), and the value for which the intensity is a maximum depends on the distance between the two minima. For the previous examples [32,33] these distances are ~ 0.6 Å and the maximum intensity takes place at Q ~ 3 $Å^{-1}$. With the TFXA spectrometer this is close to the actual value of Q for an energy transfer ~ 50 cm^{-1}. In the case of PG I the distance is shorter and the intensity maximum should occur at Q ~ 5 $Å^{-1}$. A more detailed measurement of the scattering function in the relevant Q–ω region would be necessary to measure the tunnelling transition.

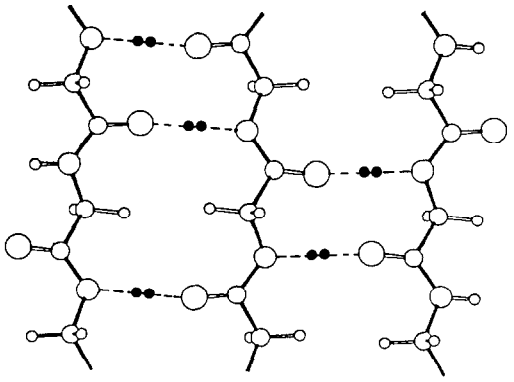

Fig. 9. Schematic representation of the antiparallel-chain rippled-sheet structure of crystalline polyglycine I. Projection on the (*a,b*) plane.

The change of the double minimum potential function along the stretching coordinate upon deuteration is spectacular. This is not unusual for strong hydrogen bonds [17,31] and a similar effect is also suspected for NMA [16]. Presumably, the effective potential for the (N)H stretching mode is not the true Born–Oppenheimer potential which should not be affected by the isotopic substitution. The localized nature of the proton vibrations is also difficult to rationalize within the Born–Oppenheimer approximation. There might be some connection between these two facts.

The symmetric double minimum observed for PG I at low temperature implies that the intra or interchain coupling between the hydrogen bonds are negligible. This is also in agreement with the absence of significant frequency dispersion in the density-of-state. This remarkable conclusion is somewhat in conflict with the intuitive picture for the proton transfer mechanism in infinite chains of hydrogen bonds. In PG I, hydrogen bonding forms a two dimensional network of delocalized protons among two equivalent sites (Fig. 9). Presumably, even weak perturbations may localize the protons on one side or the other to form either amide-like or imidol-like entities. We suppose that this sort of mechanism could play an important role in biological systems including proton transfer, even over long distances.

Hydrogen bonds between peptide units appear to be so peculiar that they could be unique, in the sense that interactions with other molecules (e.g., water) or ions will be totally different from energy, entropy and dynamics standpoints. This work emphasizes the specificity of the hydrogen bond between peptide groups. This could be an important factor in the build up of secondary structures and in the molecular recognition process.

The final picture which emerges from this work is that the structure of the peptide group is strictly intermediate between the amide-like and the imidol-like structures, which cannot be distinguished. However, the location of the double-minimum centre is unknown. It could be determined with accurate diffraction measurements. The full delocalization of the proton between the two sites and the small tunnelling related splitting observed for the amide I band mean that the geometry of the $-COCH_2N-$ entity is not changed when the proton goes back and forth between the two minima. Furthermore, the lack of intensity for the phonon wings reveals that there is virtually no dynamical interaction between the peptidic protons and the chain backbone. The situation is slightly different for NMA at low temperature where the double minimum is asymmetric and the two forms can be distinguished in this case. In addition, phonon wings give significant INS intensity for the (N)H modes. At the present stage the main factors which determine the shape of the potential function and the (non)degeneracy of the two forms are not known. The secondary structure and the nature of the side chains are probably important.

9. Conclusion

The INS spectra of three isotopic derivatives of PG I demonstrate that the peculiar proton dynamics previously observed for NMA also apply to this polypeptide. The (N)H modes are almost totally isolated from the other vibrational modes of the molecular skeleton and also from the N...O hydrogen-bond vibrations. This reveals a strong ionic character for the hydrogen bond ($N^{\delta-}...H^{+}...O^{\delta'-}$). A detailed analysis of the INS spectra with the localized-mode approach shows that (N)H-stretching frequency is split into two components at 1553 and 1377 cm^{-1}, and a new assignment scheme is proposed. In particular, the amide A and B bands are assigned to the overtones of the stretching mode. The splitting is interpreted with a symmetric double-minimum potential, in accord with the symmetry related selection rules in the infrared and Raman. This contrasts with the asymmetric potential previously

derived for NMA. Therefore, proton transfer, an essential process in biology, is achieved naturally as a result of the hydrogen bond. The dynamics is significantly changed for the N-deuterated analog. This work is a strong motivation for more detailed studies of the full scattering function, $S(Q,\omega)$, of the vibrational modes of the hydrogen-bonding protons in these systems.

10. Note added in proof

The $S(Q,\omega)$ contour map of intensity in the 2900–3000 cm^{-1} energy transfer and 0–30 $Å^{-1}$ momentum transfer range confirms the double minimum potential for the proton stretching mode in PG I at 20 K [34].

Acknowledgements

We are indebted to Mr. S.T. Robertson and Mr. M.A. Adams for their help in the neutron scattering experiments and Mr. J. Limouzi for his computing help. We should also like to thank the SERC (UK) for access to the neutron facility.

References

[1] A. Elliot and B.R. Malcolm, Trans. Faraday Soc. 52 (1956) 528.
[2] S. Suzuki, Y. Iwashita and T. Shimanouchi, Biopolymers 4 (1966) 337.
[3] M. Smith, A.G. Walton and J.L. Koenig, Biopolymers 8 (1969) 29.
[4] E.W. Small, B. Franconi and W. Peticolas, J. Chem. Phys. 52 (1970) 4369.
[5] S. Krimm and J. Bandekar, Advan. Protein Chem. 38 (1986) 181.
[6] S. Krimm, in: Biological applications of Raman spectroscopy, ed. T.G. Spiro (Wiley, New York, 1987) p. 1.
[7] K. Fukushima, Y. Ideguchi and T. Miyazawa, Bull. Chem. Soc. Japan 36 (1963) 1301.
[8] M.K. Gupta and V.D. Gupta, Indian. J. Biochem. Biophys. 13 (1976) 1.
[9] V.D. Gupta, S. Trevino and H. Boutin, J. Chem. Phys. 48 (1968) 3008.
[10] Y. Abe and S. Krimm, Biopolymers 11 (1972) 1817.
[11] A.M. Dwivedi and S. Krimm, Macromolecules 15 (1982) 177.
[12] A.M. Dwivedi and S. Krimm, Macromolecules 15 (1982) 186.
[13] A.M. Dwivedi and S. Krimm, Biopolymers 21 (1982) 2377.
[14] A.M. Dwivedi and S. Krimm, Biopolymers 23 (1984) 923.
[15] T.C. Cheam and S. Krimm, J. Chem. Phys. 82 (1985) 1631.
[16] F. Fillaux, J.P. Fontaine, M.H. Baron, G.J. Kearley and J. Tomkinson, Chem. Phys. 176 (1993) 249.
[17] F. Fillaux and J. Tomkinson, Chem. Phys. 26 (1977) 295.
[18] N. Nishi, B.I. Nakajima, N. Hasebe, and J. Noguchi, Intern. J. Biol. Macromol. 2 (1980) 53.
[19] T. Narus, B.I. Nakajima, A. Tsutsumi and N. Nishi, Polymer J. 13 (1981) 1151.
[20] J.L. Roberts and C.D. Poulter, J. Org. Chem. 43 (1973) 1549.
[21] D.G. Ott, Syntheses with stable isotopes (Wiley, New York, 1981) p. 39.
[22] J. Penfold and J. Tomkinson, Internal Report RAL-86-019, Chilton, UK (1986).
[23] S.T. Robertson, Computer Analysis of TFXA Data. Neutron Science Division (RAL, Chilton, 1988).
[24] G.J. Kearley, J. Chem. Soc. Faraday Trans. II 82 (1986) 41.
[25] L. Pauling and R.B. Corey, Proc. Natl. Aca. Sci. USA 37 (1951) 729.
[26] B. Lotz, J. Mol. Biol. 87 (1974) 169.
[27] F. Colona-Cesari, S. Premillat and B. Lotz, J. Mol. Biol. 87 (1974) 181.
[28] J. Tomkinson, in : Neutron scattering at a pulsed source, eds. R.J. Newport, B.D. Rainford and R. Cyvinski (Adam Hilger, Bristol, 1988) p. 325.
[29] A. Lautié, F. Froment and A. Novak, Spectry. Letters 9 (1976) 289.
[30] J.L. Katz and B. Post, Acta Cryst. 13 (1960) 624.
[31] A. Novak, Struct. Bonding 18 (1974) 177.
[32] F. Fillaux, A. Lautié, J. Tomkinson and G.J. Kearley, Chem. Phys. 154 (1991) 135.
[33] F. Fillaux and J. Tomkinson, Chem. Phys. 158 (1991) 113.
[34] G.J. Kearley, F. Fillaux, M.H. Baron, S. Bennington and J. Tomkinson, Science 264 (1994) 1285.